AUTOMATION IN 3D RECONSTRUCTION: RESULTS ON DIFFERENT KINDS OF CLOSE-RANGE BLOCKS

L. Barazzetti*, F. Remondino**, M. Scaioni*

* Politecnico di Milano, Department of Building Engineering Science and Technology, Milan, Italy
E-mail: (luigi.barazzetti, marco.scaioni)@polimi.it, Web: http://www.best.polimi.it
** 3D Optical Metrology Unit, Bruno Kessler Foundation, Trento, Italy
E-mail: remondino@fbk.eu, Web: http://3dom.fbk.eu

Commission V, WG V/4

KEY WORDS: 3D Modelling, Automation, Calibration, Orientation, Matching, Surface Reconstruction

ABSTRACT:
Automation in 3D reconstruction involves mainly two tasks: (i) image orientation and (ii) 3D scene reconstruction. Nowadays, automation in (i) can be considered solved for aerial photogrammetric projects, but a general and commercial solution is still pending in case of close-range image blocks. Here, the complexity and diversity of the network geometry make the automatic identification of the image correspondences a challenging task. In this paper we present a methodology to automatically orient a set of targetless close-range images taken with a calibrated camera and the following creation of 3D models with a multi-image matching algorithm. Several real cases, comprehending free-form objects (e.g. bas-relieves, decorations, etc.), building facades and images taken with UAVs are reported and discussed. Lastly, some preliminary results on a methodology for markerless camera calibration are presented.

1. INTRODUCTION

Automatic 3D reconstruction of scenes and objects from images or range data is still an open research topic. Some applications are demanding *Photosynth*-like results (Snavely *et al.*, 2008; Agarwal *et al.*, 2009) while many others are seeking highly detailed, accurate, complete, metric and photo-realistic 3D models (Levoy *et al.*, 2000; Gruen *et al.*, 2005; Remondino *et al.*, 2009). 3D models can be generated with reality-based or computer graphics methods. Reality-based approaches use real measurements and data for the geometric and appearance modelling of the surveyed scene. The actual great challenges in 3D modelling applications are: (i) the selection of the correct platform and sensor, (ii) the identification of the appropriate measurement and modelling procedure, (iii) the design of the right production workflow, (iv) the achievement of a final result in accordance with all the given initial technical specifications and (v) the possibility to fluently display and interact with the final 3D model. The most used reality-based techniques are photogrammetry and laser scanning, based respectively on passive or active optical sensors. Their integration is also providing for very good 3D modelling results in terms of completeness, accuracy and photo-realism (Stamos *et al.*, 2008; El-Hakim *et al.*, 2008; Guidi *et al.*, 2009), in particular in the case of large and complex sites. Image-based techniques are generally preferred in the case of lost objects, large monuments or architectures with regular geometric shapes, low-budget projects, good skill of the working team, time or location constraints for data acquisition and processing. Images contain all the information useful to derive the 3D shape of the surveyed scene as well as its graphical appearance (*texture*).
Generally the fundamental steps for an image-based 3D geometric reconstruction of a scene using close-range images are: (1) camera calibration, (2) image orientation and (3) 3D scene restitution. Nowadays all these steps can be performed in a fully automated way, with the level of automation as a function of the quality and accuracy of the final 3D model. The complexity and diversity of the image network geometry in close-range applications, with possible wide baselines, convergent images, illumination changes, moving objects, occlusions, variations in resolution and overlap, makes the automated identification of tie points and 3D surface reconstruction procedures more complex than in standard aerial photogrammetry.
The paper presents a methodology for the automated orientation of image blocks acquired with calibrated cameras and the successive object 3D reconstruction. The identification of the image correspondences is performed with a feature-based approach within an implemented software named *ATiPE* (Automatic Tie Point Extraction). The surface reconstruction is instead achieved with a multi-image matching approach implemented within the *CLORAMA* software. Many tests have been performed in order to validate the methodology on different datasets of images acquired with SLR or consumer grade digital cameras.

2. THE PROPOSED 3D RECONSTRUCTION PIPELINE

2.1 Image Orientation

2.1.1 Related works. Since some years, different commercial solutions utilise coded-targets for the automated camera calibration and image orientation phases (e.g. Cronk *et al.*, 2006). Targets are automatically recognised, measured and labelled to solve the identification of the image correspondences before the bundle adjustment solution. This approach becomes very useful and practical for camera calibration, but in many surveys, targets cannot be used or applied on the object to derive the exterior orientation parameters automatically. Therefore, the detection of the image correspondences is carried out with interactive measurements performed by an operator. Automated methods for tie points identification were presented in Läbe and Förstner (2006), Remondino and Ressl (2006) and Barazzetti *et al.* (2009), but a commercial solution for close-range images is still pending.

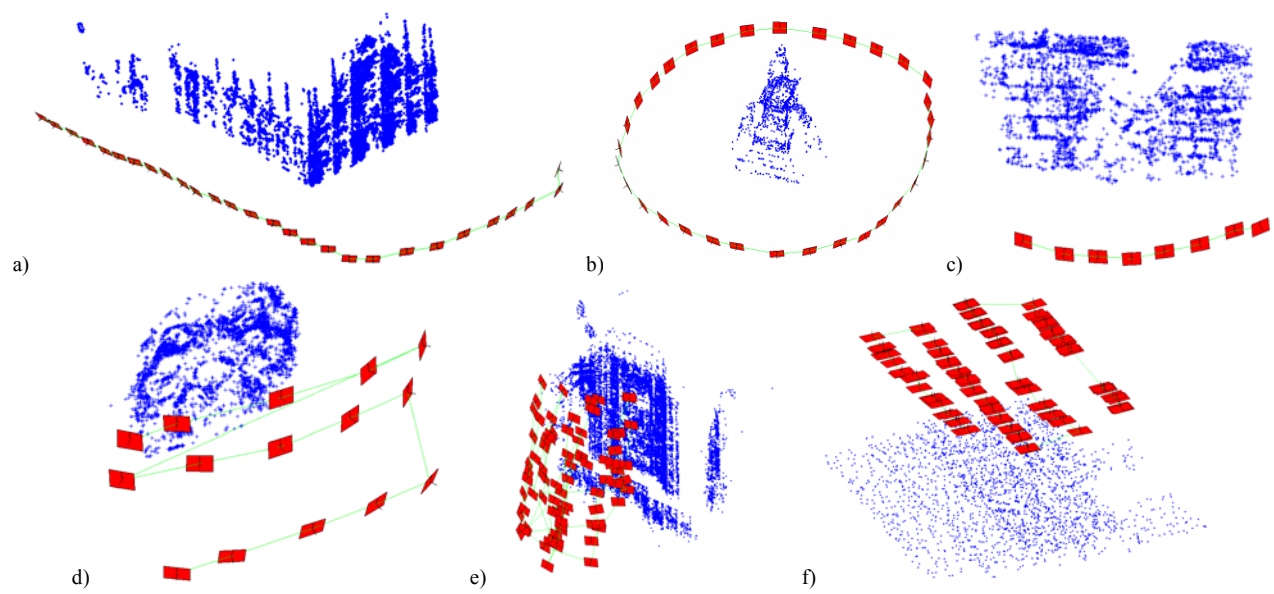

Fig. 1. Examples of close-range blocks oriented using ATiPE to automatically extract the necessary image correspondences.

Some approaches try to solve at the same time for interior and exterior orientation parameters, leading to the well known *Structure from Motion* (SfM) approach. However, such methods (Pollefeys and Van Gool, 2002; Hao and Meyer, 2003; Nister, 2004; Vergauwen and Van Gool, 2006) generally have a scarce accuracy for photogrammetric surveys. Recently the SfM concept has made great improvements, with the capability to automatically orient huge numbers of images, notwithstanding that the achievable 3D reconstructions are useful mainly for visualization, object-based navigation, annotation transfer or image browsing purpose. Two well-known packages are *Bundler* (or its graphical version *Photosynth*; Snavely *et al.*, 2008) and *Samantha* (Farenzena *et al.*, 2009). The former is the implementation of the current state-of-the-art procedures for sequential SfM applications, the latter appears even faster because of the introduction of a local bundle adjustment procedure.

2.1.2 ATiPE methodology. The developed methodology for Automate Tie Points Extraction (ATiPE) is distinguished from previous works for its flexibility, completeness of the achieved sparse point clouds and capability to process different types of images and block configurations. The robust detection of correspondences is achieved by combining the accuracy of traditional photogrammetric methods with the automation of Computer Vision approaches. The implemented feature matching strategies, coupled with an initial network geometry analysis (called *visibility map*), allow a computational time of few hours for image blocks composed of several tenth of large resolution images (more than 20 Mpx), used at their original size. A comparison between ATiPE and the state-of-the-art *Photo Tourism* (e.g. *Bundler* or *Photosynth*) is given in Table 1. The innovative aspects of ATiPE are:

- effectiveness on a large variety of unorganized and fairly large pinhole camera image datasets;
- capability to work with high resolution images;
- accurate image measurements based on the Least Squares Matching (LSM);
- combination of *feature-based* and *area-based* operators;
- strategies to derive a uniform distribution of tie points in the images;
- extension to spherical (Barazzetti *et al.*, 2010a) and multispectral (Barazzetti *et al.*, 2010b) images.

	Photo Tourism	**ATIPE**
Purpose	CV Applications	Photogrammetric Surveys
Kind of Images	Pinhole Images	Pinhole & Spherical Images
Number of images	Huge (>10 000)	Limited (a few hundreds)
Varying cameras	Yes	Yes (if calibrated)
Image size	Low resolution (compression)	High resolution with a coarse-to-fine approach
Image enhancement	None	Yes (Wallis filter)
Network geometry	Sparse block	Ad-hoc procedures for sparse blocks or sequences
Visibility information	None	Yes
Accuracy	No guarantee	Yes
Speed	Fast	Slow
Camera calibration	EXIF	EXIF or Interior with additional parameters
Matching operators	SIFT	SIFT – SURF - FAST
Detector comparison	kd-tree	Quadratic or kd-tree
Outlier rejection	**F**/**E** matrix + robust estimators	**F**/**E** matrix or homography
F/**E** estimation	8-points	7-points
Robust method	RANSAC	LMedS - RANSAC - MAPSAC
Image coordinates refining	None	LSM
Additional image points	None	Multi-image corner-based matching
Tie points reduction	None	Yes
Tie points uniform distribution	None	Yes

Table 1. Comparison of the Photo-Tourism approach (*Bundler* - *Photosynth*) and ATiPE.

A typical elaboration with ATiPE comprehends the following steps:

1) *Generation of the visibility map*. An initial network geometry analysis is carried out to roughly understand which are the connections between the images. The map is produced either

using available GPS/INS data (e.g. in case of UAV images) or with a very quick run of the entire ATiPE procedure on very low resolution images.

2) *Feature detection*. Features are extracted with the SIFT (Lowe, 2004) or with the SURF (Bay *et al.*, 2008) operator.

3) *Pairwise feature matching*. Homologous points are found by simply comparing the descriptors of the points extracted at stage (2). Two strategies can be used: (i) a *quadratic matching* procedure which ensures a good robustness but is computationally very expensive ($O(n^2)$), as all image combinations must be investigated; (ii) a *kd-tree* procedure (Beis and Lowe, 1997) based on the Approximate Nearest Neighbours (ANN) (Arya *et al.*, 1998) and the Fast Library for Approximate Nearest Neighbours (FLANN) (Muja and Lowe, 2009) libraries. Table 2 reports some results of the two implemented strategies to compare feature descriptors and extract homologous points. Both automated strategies for the comparison of the feature descriptors retrieve a sufficient number of image correspondences although some mismatches are often still present. To remove these outliers, a linear formulation and retrieval of the relative orientation (or epipolar constraint) encapsulated in the *essential* (**E**) or *fundamental* (**F**) *matrix* is used. The solution **E** (or **F**) is sought with robust techniques (RANSAC, LMedS or MAPSAC are available) to face the presence of outliers.

			kd-tree		*quadratic*	
Image size	*Features image1*	*Features image 2*	*Matched features*	*Time (s)*	*Matched features*	*Time (s)*
640×480	1391	1405	262	2	328	3
1500×1004	5636	5017	349	6	419	19
2816×2112	23080	22806	1204	39	1690	465
3072×2304	21343	20691	2018	59	2936	698
4500×3000	83729	87471	19336	162	27772	7900
5616×3744	94208	127359	25968	339	34230	22580

Table 2. Comparison between quadratic- and "kd-tree"-based matching strategies.

4) *Image concatenation*. Once the correspondences between image pairs are robustly extracted the method tries to link all the images together. Different strategies are followed according to the block structure: for *ordered image sequences* (Fig. 1 a,b,c) the whole sequence is divided into *n*-2 triplets in order to determine the correspondences inside each triplet. After the single triplet matching, the image coordinates of consecutives triplets are compared among them to match the correspondences along the whole sequence. In the case of closed circuits the method can create an additional triplet to correctly close the sequence. This method has a linear computational cost $O(n)$ with respect to the number of images. For *unordered sets* of images (Fig. 1 d,e,f) it is necessary to check all possible image pair combinations to determine the ones sharing sufficient correspondences. Therefore each image must be compared with all the others, leading to a high computational cost $O(n^2)$. For this reason, the use of the *visibility map* is recommended.

5) *Image coordinates refinement*. The image coordinates of homologous points extracted using operators like SIFT or SURF generally do not allow the derivation of highly accurate orientation results. Therefore to improve the location accuracy of the image coordinates a LSM refining is applied to full resolution images. In the case of widely separated and convergent images, the descriptor values can be even used as initial approximation of the LSM parameters (Remondino and Ressl, 2006). A successive improvement is achieved using the FAST operator (Rosten and Drummond, 2006) which demonstrated to quickly extract a large number of corners under a higher repeatability compared to SIFT and SURF, with also a better distribution in the images and a higher accuracy of the final sparse geometry (Jazayeri and Fraser, 2010).

6) *Reduction and regularization of tie point distribution*. High resolution images picturing objects with a good texture generally generate a huge number of image correspondences, which are very often not uniformly distributed in the images. This can cause low accuracy results and very long processing time. Therefore, each image is divided into rectangular cells where only the features with the largest multiplicity are used. A significant reduction of the correspondences (even more than 100 times) is achieved, preserving the accuracy of the final product. Secondly, as the features are generally random-distributed in the images without a uniform distribution (Fig. 2), the method improves also the geometric distribution of the correspondences. Consequently, the quality of the final results is increased in terms of geometric distribution of tie points and reduction of both processing time and computational cost.

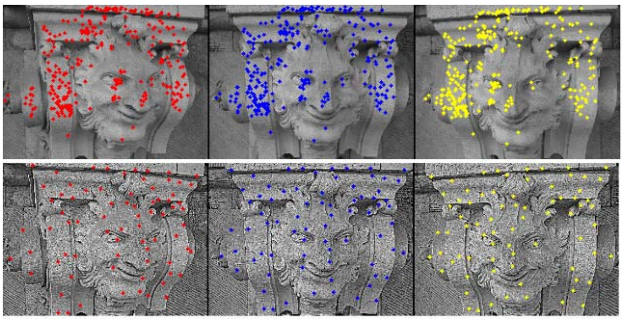

Fig. 2. Random and non-uniform distribution of the features extracted with SIFT (above). Derived uniform distribution of the correspondences obtained with the proposed approach (below).

The typical output of ATiPE contains the pixel coordinates of all the homologous points, which can be then imported and used for image orientation and sparse geometry reconstruction in most commercial photogrammetric software (e.g. *Australis*, *iWitness*, *iWitnessPro*, *Leica Photogrammetry Suite*, *PhotoModeler*, *Bundler*).

2.2 Scene reconstruction

After the image orientation achieved coupling the output of ATiPE with any bundle adjustment solution, according to the imaged scene and contents, a fully automated or interactive 3D reconstruction of the scene is performed. For architectural structures with well defined and repeated geometric primitives (e.g. buildings), interactive methods are still more powerful and reliable than automated surface reconstruction algorithms. On the other hand, in the case of free-form objects, like bas-relieves, decorations, ornaments, statues, dense and detailed point clouds are more useful. The recent developments in automated image correlation (Furukawa and Ponce, 2007; Goesele *et al.*, 2007) have shown the great potentialities of the approach, with 3D results very similar to active sensors (Remondino *et al.*, 2008).

In our methodology, the *CLORAMA* procedure was employed for the generation of accurate and dense point clouds from oriented images. *CLORAMA* implements a multi-image matching technique based on the Multi-Photo Geometrically Constrained (MPGC) concept of Gruen and Baltsavias (1988).

The matching algorithm was originally developed by Zhang and Gruen (2004) and then adapted and extended to terrestrial convergent images (Remondino *et al.*, 2008). Now the software (*CLORAMA*) is offered by the ETH Zurich spin-off 4DiXplorer (www.4dixplorer.com).
The derived dense point clouds are then converted into structured mesh using commercial packages. The surface model is automatically textured using the known camera parameters and one or multiple images. In the image overlapping areas, blending is performed to get seamless texture and photo-realistic results.

3. EXPERIMENTS

3.1 3D modeling of free-form objects

The developed methodology was tested with several free-form objects obtaining satisfactory results in terms of accuracy and completeness of the achieved reconstructions. This kind of objects normally have a good texture for the preliminary feature-based matching and the following surface reconstruction phase. Some results are shown in figures 3 and 4, where the whole elaboration time took around 3 hours for each object.

Fig. 3. A surface model (shown in color-shaded and textured mode) was derived in approximately 3 hours from a sequence of 8 images.

Fig. 4. Automated 3D reconstruction of a marble bass-relief (ca 1.5 m width) modelled from 5 images. The dense matching of CLORAMA produced a DSM with a 1 mm grid resolution and ca 2.3 million points.

3.2 Architectural reconstruction

Although the exterior orientation parameters of a set of images used for the 3D restitution of architectures can be computed fully automatically, the successive automatic 3D metric restitution of building facades or complex architectures is still a challenging task. Hence most of the 3D reconstructions are done with interactive measurements (Patias *et al.*, 2008). In fact, interactive methods still remain the best approach as several elementary surfaces or solids can be grouped together to create 3D models of the object. Fully automated procedures normally produce dense 3D point clouds useful mainly for visualization purposes at small or medium scale but are not ideal for detailed surveying or architectural drawings.
The reported procedure was tested with the main façade of the Sanctuary of Re (Valle Vigezzo, Italy). The survey was carried out with a calibrated SLR Nikon D700 camera with a 20 mm lens. 13 images were taken and then oriented in a few minutes using the SURF operator and a *kd-tree* search (Fig. 5). We verified that the geometry of the building façade, with several repetitive elements and symmetries, generated some outliers during the descriptor-based matching of the SURF keypoints. This unwanted effect was also found for other building facades, demonstrating a potential limit for an automated matching procedure. Robust estimators used to derive the **E** or **F** matrix work with image pairs, therefore mismatches lying on the epipolar line cannot be rejected. However, the use of a robust photogrammetric bundle solution helped to remove the mismatches using rejection criteria and the combined use of several images per point. Furthermore, the number of images was reduced of 50% (7 images) to check the performances of ATiPE. Lastly, an additional reduction (4 images) was applied. Even in this case, with larger baselines, the orientation of the images could be computed fully automatically.
After the image orientation, the interactive restitution of the architectural façade took almost one day to derive the textured model shown in Fig. 5.

	13 images	***7 images***	***4 images***
Sigma naught (px)	0.69	0.62	0.90
RMS (px)	0.74	0.63	0.81
3D points	2,852	875	42

Table 3. Some results in the case of a progressive image reduction.

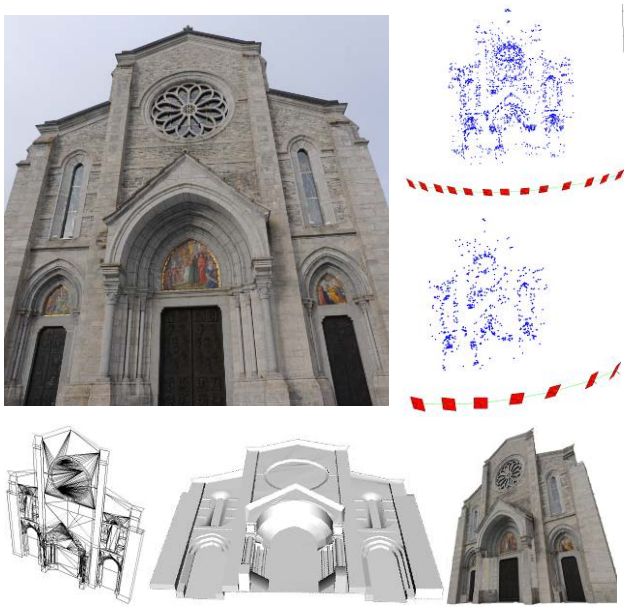

Fig. 5. A sanctuary façade and the camera poses with the sparse 3D point cloud (above). At the bottom the produced geometric 3D model of the church façade is shown.

3.3 ATiPE for typical SfM projects

The automated orientation procedure was also tested on large data sets of images acquired with calibrated consumer digital cameras. In figures 6 and 7 the results on “Piazza del

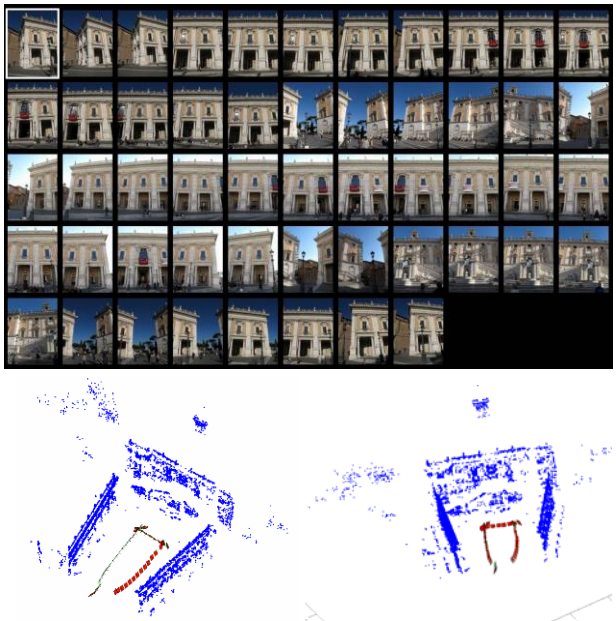

Fig. 6. The "Piazza del Campidoglio" sequence, made up of 52 images. The bundle adjustment derived a sparse point cloud of ca 11,800 3D points.

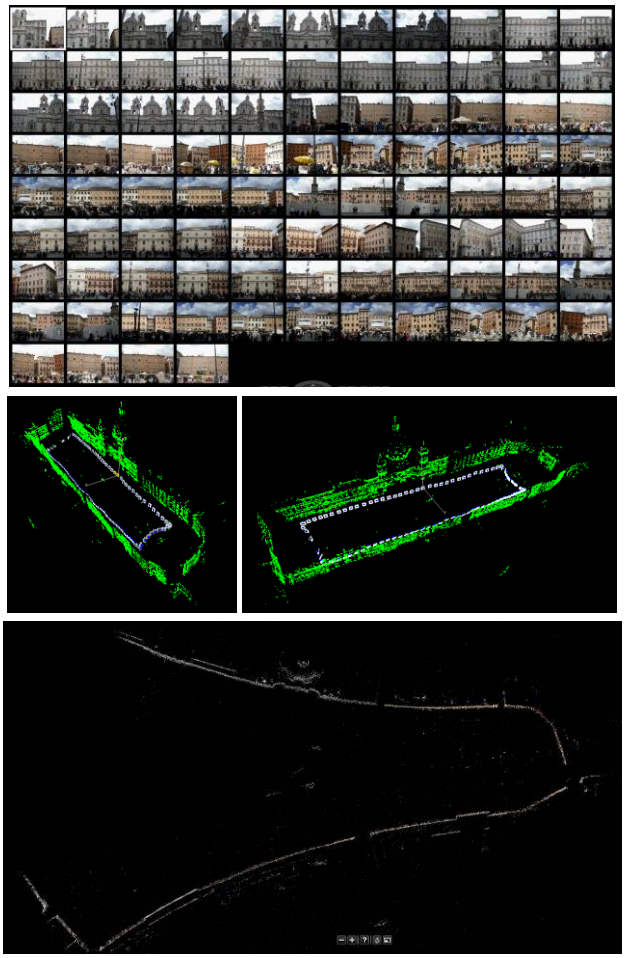

Fig. 7. The "Piazza Navona" sequence, with 92 images automatically oriented in 5 hours deriving a sparse point cloud of ca 18500 3D points. At the bottom, the orientation results achieved using Photosynth: the adjustment diverged and failed to close the sequence.

Campidoglio" and "Piazza Navona" (Rome, Italy) are shown, while Table 4 reports the main characteristics of the two large image blocks. The "Piazza Navona" sequence was also oriented using Photosynth, which produced the network shown at the bottom of figure 7. In this case the adjustment diverged and was not able to close the sequence with a result far away from the correct solution.

For the 3D reconstruction of the buildings in the figures, interactive procedures would be the best approach in order to produce complete and detailed architectural 3D models.

	Piazza del Campidoglio	***Piazza Navona***
# images	52	92
Image resolution	4,416×3,312 px	4,000×3,000 px
3D tie points	11,772	18,489
Final RMS	1.20 px	0.79 px

Table 4. Main characteristics of the two large datasets oriented using ATiPE to automatically extract the image correspondences.

3.4 3D modeling from UAV images

The developed methodology is also useful for the analysis and automated orientation of images taken with mini-helicopters. The case studies considered in this section are two UAV flights over the archaeological area of Copan (Honduras). The images were taken with a calibrated 12 Mpx SLR camera and the blocks have a regular geometry with several strips.

The first image block (Fig. 8) is composed of 70 images over the East Court of the site. The block was elaborated with the SIFT operator and a *kd-tree* search removing the outliers with the MAPSAC approach. An initial *visibility map* was created using low resolution images to reduce the number of image combinations. The feature-based matching phase provided more than 57,000 image points, which were then used to determine the exterior orientation parameters. The free-network bundle solution gave an RMS of 3.4 μm (pixel size is 5.5 μm) and 27,548 3D points. 122 points were considered as outliers and automatically rejected. After the procedure for image point reduction, ATiPE provided 6,498 points and the new bundle solution gave an RMS of 3.1 μm, with 1,127 3D points and only 23 outlier. As can be seen, there is no loss of precision and the elaboration became much faster.

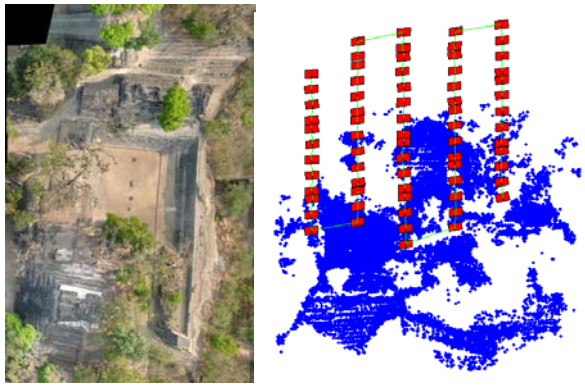

Fig. 8. A mosaic over the East Court (left) and the oriented image block composed of 70 UAV images.

The second image block (Fig. 9) is composed of 18 images over the Main Plaza. The photogrammetric bundle solution provided a final RMS equal to 0.49 px and 12,090 3D points. For some archaeological structures and for documentation and visualization purposes, an automated 3D reconstruction of some pyramidal structures was achieved using the *CLORAMA* image matcher (Fig. 10).

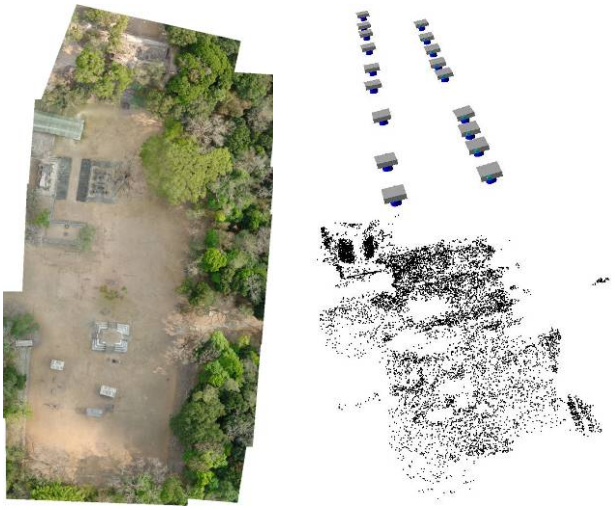

Fig. 9. An overview of the Main Plaza in Copan, Honduras (left). The recovered camera poses and 3D points (ca 6500) after the automated orientation of the 18 UAV images (right) of block (2).

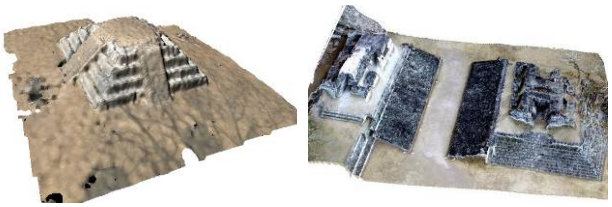

Fig. 10. Automated 3D reconstruction of some man-made structures using advanced image matching techniques.

3.5 Targetless camera calibration

Camera calibration is a fundamental prerequisite for accurate measurements from images. The performances of ATiPE were tested also for a targetless camera calibration procedure, using 30 images acquired with a Nikon D200 (3,872×2,592 px, pixel size of 6.1 μm) with a 20 mm Nikkor lens. To compare the results with the current state-of-the-art approach, *iWitness* (Photometrix) calibration targets were also placed in the scene (Fig. 11). ATiPE was run using the SURF operator. The self-calibrating bundle adjustment performed in *Australis* (Photometrix) with and without coded targets provided the results reported in Table 5. It is evident how the adjustment results are pretty similar. The main issue is related to the elaboration time (few seconds with the coded targets, several hours with the natural features) but several improvements can be carried out to improve the computational performances of the method.

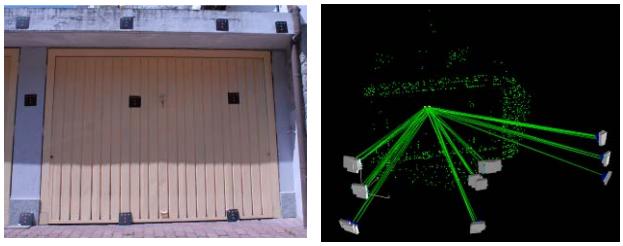

Fig. 11. The scene used for the automated camera calibration with and without coded targets (left). The camera network of the targetless solution with the recovered camera poses and sparse point cloud (right).

	With targets (iWitness colour targets)	Without targets (natural features)
RMS	0.16 px	0.59 px
Focal	20.436 mm (0.003mm)	20.424 mm (0.003mm)
PP x	0.051 mm (0.003mm)	0.076 mm (0.002mm)
PP y	0.051 mm (0.003mm)	0.048 mm (0.002mm)
K1	2.8173e-004 (2.605e-006)	2.7331e-004 (2.510e-006)
K2	-4.5538e-007 (3.585e-008)	-4.6780e-007 (2.666e-008)
K3	-2.7531e-010 (1.452e-010)	-5.8892e-011 (9.253e-011)
P1	7.849e-006 (2.11e-006)	1.994e-006 (1.98e-006)
P2	-1.6824e-005 (2.25e-006)	-1.436e-005 (1.86e-006)

Table 5: Results of the automated camera calibration performed with and without targets: estimated values and their precisions.

4. CONCLUSIONS

The article presented an automated methodology for close-range image orientation and, in the case of free-form objects, dense and detailed 3D surface reconstruction. We demonstrated that automated image orientation and surface measurement are nowadays achievable with satisfactory results in terms of accuracy and geometric models. For more performance analyses and accuracy results we remand to (Barazzetti *et al.*, 2009).

The geometric accuracy is getting more and more important while nice-to-look-at visual results are no more sufficient besides visualization purposes or VR applications. The presented procedure combines algorithms and benefits from Computer Vision and Photogrammetry and allows the generation of textured 3D models from calibrated image blocks or sequences. ATiPE includes SIFT and SURF detectors/descriptors for a preliminary orientation and uses the FAST interest operator and the LSM technique to achieve more accurate image locations. Moreover, ATiPE derives orientation results with the same accuracy of classical and generally more reliable manual measurements. The achieved orientation results are the base for the successive automated multi-image surface measurement performed with the *CLORAMA* matcher.

Photogrammetry is therefore increasing its capabilities and potentialities regarding the automation of the image processing and scene reconstruction, but still keeping the accuracy of the results as primary goal.

REFERENCES

References from Journals

Arya, S., Mount, D.M., Netenyahu, N.S., Silverman, R. and Wu, A.Y., 1988. An optimal algorithm for approximate nearest neighbour searching fixed dimensions. Journal of the ACM, 45(6): 891-923.

Bay, H., Ess, A., Tuytelaars, T., Van Gool, L., 2008. SURF: Speeded up Robust Features. *CVIU*, 110(3): 346-359.

Cronk, S., Fraser, C.S., Hanley, H.B., 2006. Automatic Calibration of Colour Digital Cameras. Photogrammetric Record, 21(116): 355-372.

Gruen, A., and Baltsavias, E.P., 1988. Geometrically constrained multiphoto matching. Photogrammetric Engineering and Remote Sensing, 54(5): 633-641.

Guidi, G., Remondino, F., Russo, M., Menna, F., Rizzi, A., Ercoli, S., 2009: A multi-resolution methodology for the 3D modeling of large and complex archaeological areas. Int. Journal of Architectural Computing, 7(1): 40-55.

Jazayeri, I. and Fraser, C., 2010: Interest operators for feature-based matching in close range photogrammetry. The Photogrammetric Record, 25(129): 24-41.

Lowe, D., 2004: Distinctive image features from scale-invariant keypoints. Int. Journal of Computer Vision, 60(2): 91-110.

Pollefeys, M., Van Gool, L., 2002: From images to 3D models. Communications of the ACM, 45(7): 50-55

Remondino, F., El-Hakim, S., Gruen, A., Zhang, L., 2008: Turning Images into 3-D Models - Development and performance analysis of image matching for detailed surface reconstruction of heritage objects. IEEE Signal Processing Magazine, 25(4): 55-65.

Snavely, S.M., Seitz, R., Szelinski, R., 2008: Modelling the world from internet photo collections. Int. Journal of Computer Vision, 80(2): 189-210.

Stamos, I., Liu, L., Chen, C., Woldberg, G., Yu, G. And Zokai, S., 2008: Integrating automated range registration with multiview geometry for photorealistic modelling of large-scale scenes. Int. Journal of Computer Vision, 78(2-3): 237-260.

Vergauwen, M., Van Gool, L.J, 2006: Web-based reconstruction service. Machine Vision and Applications, 17(6): 411-426.

References from Other Literature

Agarwal, S., Snavely, N., Simon, I., Seitz, S.M., Szeliski, R., 2009: Building Rome in a Day. Proc. ICCV 2009, Kyoto, Japan.

Barazzetti, L. Remondino, F., Scaioni, M., 2009: Combined use of photogrammetric and computer vision techniques for fully automated and accurate 3D modeling of terrestrial objects. Videometrics, Range Imaging and Applications X, Proc. of SPIE Optics+Photonics, Vol. 7447, 2-3 August, San Diego, CA, USA.

Barazzetti, L., Remondino, F., Scaioni, M., Lo Brutto, M., Rizzi. A., Brumana, R., 2010: Geometric and radiometric analysis of paintings. International Archives of the Photogrammetry, Remote Sensing and Spatial Information Sciences, Vol. 39(5), Newcastle, UK (in press).

Beis, J. and Lowe, D., 1997: Shape indexing using approximate nearest neighbour search in high dimensional spaces. Proceedings of Computer Vision and Pattern Recognition, pp. 1000-1006.

El-Hakim, S., Beraldin, J.-A., Remondino, F., Picard, M., Cournoyer, L., Baltsavias, M., 2008: Using terrestrial laser scanning and digital images for the 3D modelling of the Erechteion, Acropolis of Athens. Proc. of "Digital Media and its Applications in Cultural Heritage" (DMACH) Conference, pp. 3-16, Amman, Jordan.

Farenzena, M., Fusiello, A., Gherardi, R., 2009: Structure and Motion pipeline on a hierchical cluster tree. Proc. of IEEE 3DIM Conference, Kyoto, Japan.

Furukawa, Y., Ponce, J., 2007: Accurate, Dense, and Robust Multi-View Stereopsis. Proc. CVPR 2007.

Goesele, M., Snavely, N., Curless, R., Hoppe, H. And Seitz, S.M., 2007: Multi-view stereo for community photo collections. Proc. ICCV 2007, Rio de Janeiro, Brazil.

Gruen, A., Remondino, F., Zhang, L., 2005: The Bamiyan project: multi-resolution image-based modeling. In Recording, Modeling and Visualization of Cultural Heritage. E.Baltsavias, A.Gruen, L.Van Gool, M. Pateraki (Eds), Taylor & Francis / Balkema, 2005, ISBN 0-415-39208-X, pp. 45-54.

Hao, X., Mayer, H., 2003: Orientation and auto-calibration of image triplets and sequences. International Archives of the Photogrammetry, Remote Sensing and Spatial Information Sciences, 34(3-W8): 73-78.

Läbe, T., Förstner,W., 2006. Automatic relative orientation of images. Proceedings of the 5th Turkish-German Joint Geodetic Days, Berlin, Germany.

Levoy, M., Pulli, K., Curless, B., Rusinkiewicz, S., Koller, D., Pereira, L., Ginzton, M. Anderson, S., Davis, J., Ginsberg, J., Shade, J., Fulk, D., 2000: The digital michelangelo project: 3d scanning of large statues. SIGGRAPH Computer Graphics Proceedings, pp. 131-144.

Muja, M. and Lowe, D., 2009. Fast approximate nearest neighbours with automatic algorithm configuration. International Conference on Computer Vision Theory and Applications (VISAPP'09), 10 pp.

Nister, D., 2004. Automatic passive recovery of 3D from images and video. In: proc. of the 2nd IEEE Int. Symp. on "3D data processing, visualization and transmission", pp. 438-445.

Patias P. Grussenmeyer P., Hanke K., 2008: Applications in cultural heritage documentation. In "Advances in Photogrammetry, Remote Sensing and Spatial Information Sciences", 2008 ISPRS Congress Book, 7, pp. 363-384.

Remondino, F., Ressl, C., 2006: Overview and experience in automated markerless image orientation. IAPRSSIS, 36(3): 248-254.

Remondino, F., El-Hakim, S., Girardi, S., Rizzi, A., Benedetti, S. And Gonzo, L., 2009: 3D Virtual reconstruction and visualization of complex architectures - The 3D-ARCH project. International Archives of the Photogrammetry, Remote Sensing and Spatial Information Sciences, Vol. 38(5/W1), Trento, Italy (on CD-Rom).

Rosten, E. and Drummond, T., 2006: Machine learning for high-speed corner detection. Proceedings of the European Conference on Computer Vision, Graz, Austria, pp. 430-443.

Zhang, L. and Gruen, A., 2004: Automatic DSM generation from linear array imagery data. International Archives of the Photogrammetry, Remote Sensing and Spatial Information Sciences, 35(3), pp. 128-133.